

Local probing of coupled interfaces between two-dimensional electron and hole gases in oxide heterostructures by variable-temperature scanning tunneling spectroscopy

M. Huijben,^{*} D. Kockmann, J. Huijben, J. E. Kleibeuker, A. van Houselt, G. Koster, D. H. A. Blank, H. Hilgenkamp, G. Rijnders, A. Brinkman, and H. J. W. Zandvliet

Faculty of Science and Technology and MESA⁺ Institute for Nanotechnology, University of Twente, P.O. BOX 217, 7500 AE Enschede, The Netherlands

(Received 28 October 2011; revised manuscript received 1 July 2012; published 24 July 2012)

The electronic structure of an epitaxial oxide heterostructure containing two spatially separated two-dimensional conducting sheets, one electronlike (2DEG) and the other holelike (2DHG), has been investigated using variable temperature scanning tunneling spectroscopy. Heterostructures of LaAlO₃/SrTiO₃ bilayers on (001)-oriented SrTiO₃ (STO) substrates provide the unique possibility to study the coupling between subnanometer spaced conducting interfaces. The band gap increases dramatically at low temperatures due to a blocking of the transition from the conduction band of the STO substrate to the top of the valence band of the STO capping layer. This prevents the replenishment of the depleted electrons in the capping layer from the underlying 2DEG and enables charging of the 2DHG by applying a negative sample bias voltage within the band gap region. At low temperatures the 2DHG can be probed separately with the proposed experimental geometry, although the 2DEG is located less than 1 nm below.

DOI: [10.1103/PhysRevB.86.035140](https://doi.org/10.1103/PhysRevB.86.035140)

PACS number(s): 73.20.-r, 73.40.Gk

I. INTRODUCTION

Following the discovery¹ of novel two-dimensional electron gas/liquid behavior occurring at interfaces between insulating oxides, such as SrTiO₃ (STO) and LaAlO₃ (LAO), many studies have revealed the rich phenomenology of these conducting states²⁻⁴ and the potential for novel device structures on length scales smaller than attainable with standard semiconductors.^{5,6} A key ingredient underlying the conductivity appears to be the polar discontinuity across the interface between the polar LAO and the nonpolar STO. This is conceived to result in an electrostatic potential buildup in the LAO, causing a transfer of electrons from the surface, across the LAO layer, into the STO conduction band. In addition to this electronic reconstruction induced doping, also extrinsic sources are found to contribute to the interface behavior, such as oxygen and cation vacancies⁷⁻⁹ or cation intermixing.¹⁰⁻¹²

For LAO films grown on TiO₂-terminated STO substrates, an insulator to metal transition was found when the LAO film exceeds a thickness of 3 unit cells.¹³ This is in line with the understanding that a critical LAO thickness is needed to acquire a sufficiently strong potential buildup to drive the charge transfer. Remarkably however, when a STO capping layer is grown on top of the LAO film, metallic behavior is seen already for a single LAO unit cell thickness.¹⁴ This was interpreted as the result of a surface dipole effect in the STO,¹⁵ contributing to the potential buildup.¹⁶ A tantalizing consequence following from this is the occurrence of a two-dimensional hole gas (2DHG) at the STO surface formed by oxygen *2p* states from which electrons have been transferred to the two-dimensional electron gas (2DEG) at the STO-LAO interface underneath. This would imply a parallel configuration of a two-dimensional electron conductor and a two-dimensional hole conductor, see Fig. 1, at a distance of only about 2 perovskite unit cells (uc), which is less than 1.0 nm. Such a situation is reminiscent to coupled 2DEG/2DHG systems in semiconductor heterostructures, in that case at typical distances of several tens of nm, in which,

for example, exciton formation and their potential Bose-Einstein condensation are studied.^{17,18} Key to the occurrence of excitons in such bilayer 2D systems is minimizing the separation distance to achieve strong Coulomb interaction, while maintaining a small probability of recombination by their spatial separation.

Evidence for the occurrence of parallel conducting sheets (2DEG and 2DHG) in STO(001)/LAO/STO heterostructures was provided by magnetotransport studies and ultraviolet photoelectron spectroscopy,¹⁶ which demonstrated macroscopically the presence of electrons as well as holes. However, the spatial separation of conducting sheets with exclusively electrons or holes as carriers could not be determined yet. Here, we report on the local characterization of the electronic structure of closely coupled 2DEG and 2DHG interfaces by STM and STS experiments on STO-capped LAO layers on STO(001) substrates, revealing the individual interface (2DEG) and surface (2DHG) conducting sheets including their temperature dependent coupling.

II. EXPERIMENT

A. Unit cell controlled growth process

The epitaxial STO(001)/(2 unit cell LAO)/(1 unit cell STO) heterostructures used for these studies were fabricated by pulsed laser deposition (PLD) with reflection high-energy electron diffraction (RHEED) control of the growth process. Preparation by a combined HF-etching/anneal treatment¹⁹ is expected to result in atomically smooth TiO₂-terminated SrTiO₃ (100) substrates, which enables unit cell controlled growth of individual oxide layers.²⁰ All substrates had vicinal angles of $\sim 0.1^\circ$. Single crystal STO(001) and LAO(001) targets were ablated at a laser fluence of ~ 1.3 J/cm² and a repetition rate of 1 Hz. The substrate was held at 850 °C during deposition of both layers, while an oxygen pressure of 2×10^{-3} mbar was used. RHEED analysis demonstrates the preservation of the (1 × 1) surface reconstruction from the initial TiO₂-terminated

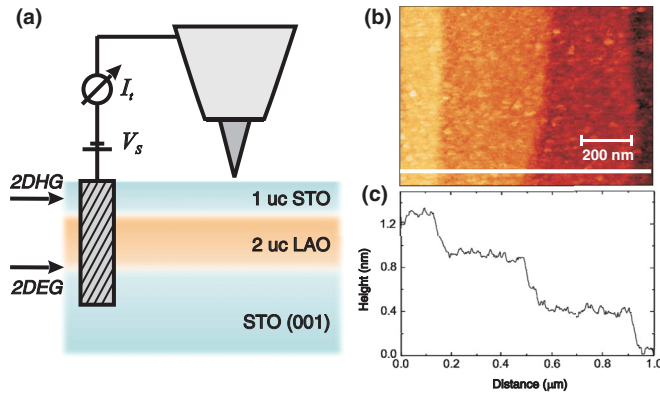


FIG. 1. (Color online) (a) Schematic representation of the experimental geometry. Two spatially separated two-dimensional (2D) conducting sheets, one electronlike (2DEG) and the other holelike (2DHG), are considered to be created at the interfaces in STO(001)/LAO/STO heterostructures. Temperature dependent scanning tunneling microscopy (STM) and spectroscopy (STS) are performed by monitoring the tunneling current I_t between the tip and the sample as a function of V_s , voltage at the sample relative to the tip. (b) Surface topography image and (c) corresponding height profile recorded by STM at -1.0 V and 300K.

STO (100) substrate²¹ surface to the final surface of the STO top layer.²⁰

To demonstrate the high level of control and reproducibility of the growth procedure, RHEED intensity analysis is shown in Fig. 2 of the growth of two SrTiO₃(001)/(2 uc LaAlO₃)/(1 uc SrTiO₃) heterostructures. Identical characteristics were observed in the RHEED analysis displaying the reproducibility of RHEED-assisted pulsed laser deposition. The deposition of LaAlO₃ was stopped exactly in the second maximum of the RHEED intensity, indicating the growth of two unit cells. The deposition of the SrTiO₃ top layer was interrupted after a single unit cell. However, one extra laser pulse, more than required for the maximum of the RHEED intensity oscillation, was

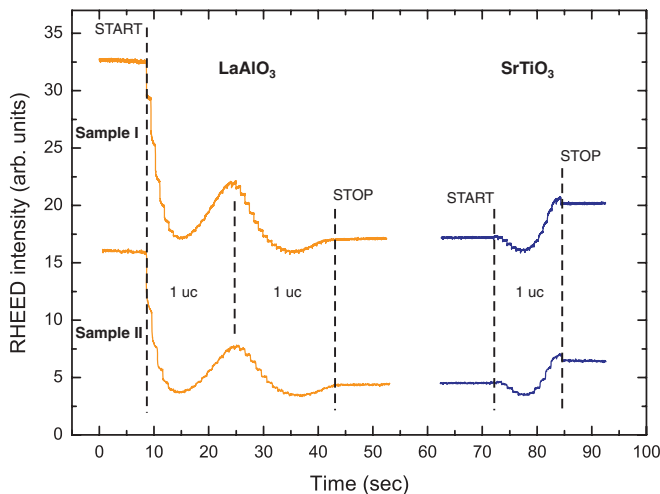


FIG. 2. (Color online) RHEED intensity analysis during epitaxial growth of two SrTiO₃(001)/(2 uc LaAlO₃)/(1 uc SrTiO₃) heterostructures by RHEED-assisted pulsed laser deposition showing identical characteristics.

given to be certain that the SrTiO₃ top layer was fully closed. This can be observed in Fig. 2 where the intensity after the last laser pulse is slightly lower than the intensity of the maximum.

After growth, the heterostructures were slowly cooled to room temperature in the oxygen deposition pressure at a rate of 10 °C/min. As a counter electrode for the STM/STS experiments, aluminum wire bonds have been used, forming a shared contact to both interfaces separated a few mm from the investigated area; see Fig. 1. We note that for such thin stacks, contacting the conducting interfaces/surfaces separately is experimentally very challenging. Subsequently, the heterostructures were transferred through air to an ultrahigh vacuum variable temperature cryostat for STM and STS analysis without any intermediate heating or etching procedure.

B. STS spectrum recording procedure

The scanning tunneling microscopy and spectroscopy experiments are performed with an Omicron ultrahigh vacuum low temperature STM system, which has a base pressure of 3×10^{-11} mbar. Therefore any contamination during the measurements can be safely disregarded. We have used electrochemically etched tungsten STM tips for all our experiments. The temperature was varied from 77 to 300 K. The sample bias and initial tunneling current set points were always kept below 4 V and 4 nA, respectively. The $I(V)$ experiments are performed by presetting the sample bias and the tunneling current, and with this the tip-sample separation, at an initial value and subsequently measuring I as a function of V with the feedback disabled,²² i.e., with the tip-sample separation fixed.

The IV curves are averaged over the entire 30×30 nm² scans. Each scan involves 100 IV traces, taken in a 10×10 grid. The variation from trace to trace is marginal. The STS measurements were recorded as follows. Before opening the feedback loop a delay of 200 μ s was used. After opening the feedback loop, the voltage was kept constant at the set point and a delay of 50 μ s was applied. At each voltage point the current was measured for 640 μ s, followed by a delay of 50 μ s. After every change in bias voltage, a delay of 80 μ s was applied. Before closing the loop again a delay of 100 μ s was applied and after closure of the feedback loop a delay of 50 μ s was applied before continuing the scanning. So in total, including the normal scanning, this amounts to about 4 minutes for a 30×30 nm scan (200×200 points measurements with a 10×10 STS grid). The differential conductance dI/dV was extracted numerically from the $I(V)$ curve. In order to check the quality of our dI/dV data, we have also measured the differential conductivity using a lock-in technique. The normalized differential conductance $(dI/dV)/(I/V)$ is known to resemble the local density of states (LDOS) of the surface,^{22,23} whereby it should be noted that at the Fermi level (where $V = 0$) the normalized differential conductance is always 1. As is clear from Fig. 3, the exact shape of the LDOS spectrum depends on the actual value of the set points.

III. RESULTS

The low level of surface roughness of our samples was confirmed by scanning tunneling microscopy analysis of the surface (Fig. 1), exhibiting smooth terraces separated by clear

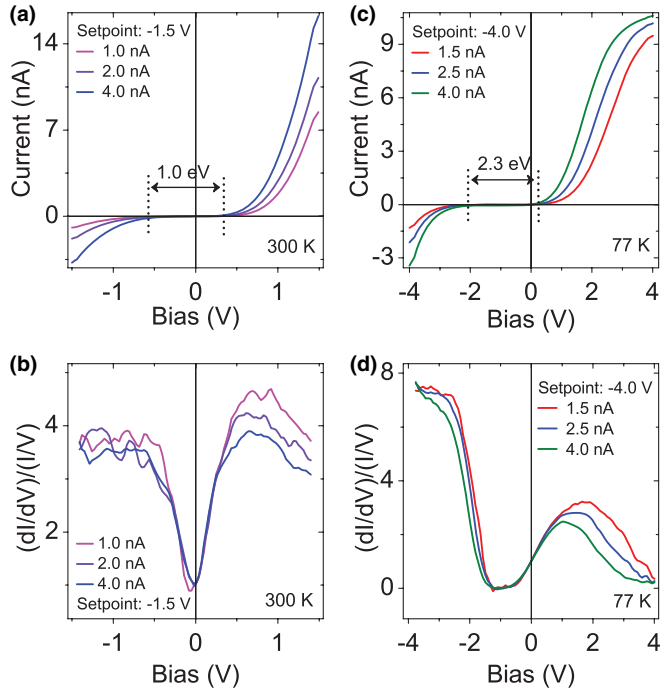


FIG. 3. (Color online) IV curves and LDOS, $(dI/dV)/(I/V)$ of the STO(001)/2LAO/1STO heterostructure, recorded at (a), (b) 300 and (c), (d) 77 K.

unit cell height steps similar to the surface of the initial STO (001) substrate. It is noted that for the STO capping layer about 8% more PLD pulses than required for a single unit cell were used to ensure the presence of a fully closed STO capping layer, which explains the presence of small clusters in the STM images. In Fig. 3 the scanning tunneling spectroscopy data of the STO(001)/2LAO/1STO heterostructure at 300 and 77 K are shown. Different initial set points were chosen at both temperatures to provide a bias voltage larger than the band gap. The most remarkable features are the increase of the band gap from about 1.0 eV at 300 K [Fig. 3(b)] to approximately 2.3 eV at 77 K and the increasing asymmetry at low temperatures. At 77 K this band gap is predominantly in the energy range below the Fermi level, as is common for n-type conducting behavior.

The typical tunneling currents in our experiments are significantly higher than observed for STM/STS studies on uncapped 4 uc LAO layers on STO, as reported by Breitschaft *et al.*²⁴ and Ristic *et al.*²⁵ This supports the conjecture that in our STO-capped system the surface is conducting as well. In addition, the observation of high tunneling currents at positive sample biases, for the room temperature scans, is in line with a predominant tunneling from a 2D hole gas, as predicted to be present at the STO surface.

Density functional theory (DFT) calculations of the band structure¹⁶ of the STO(001)/2LAO/1STO heterostructure are shown in Fig. 4. The valence band maximum is defined by the O 2p states at the M point in the STO surface layer, while Ti 3d states at the LAO-STO substrate interface mark the bottom of the conduction band, located at the Γ point of the Brillouin zone. The indirect band gap for this system was calculated to be ~ 0.3 eV, while the direct band gap at the Γ points was ~ 0.8 eV.

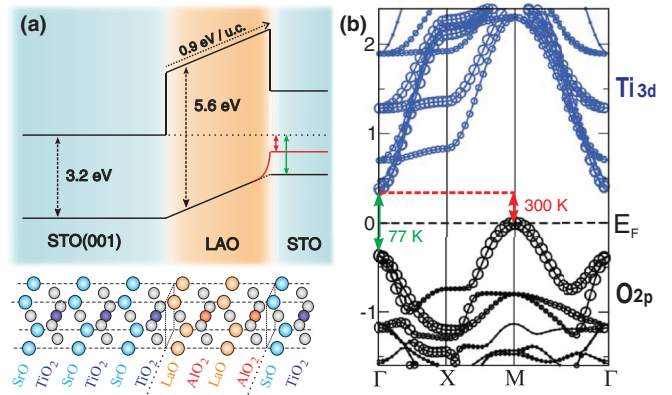


FIG. 4. (Color online) (a) Schematic representation and (b) DFT calculation of the band structure of the STO(001)/2LAO/1STO heterostructure with band gaps at 300 and 77 K. Data taken from Ref. 16.

It should be noted though that DFT calculations typically underestimate band gaps. The small band gap experimentally observed at 300 K suggests that at this temperature both the surface (M point) as well as the interface states (Γ point) are probed. At cryogenic temperatures, however, the tunneling from the STM tip to the finite k -value STO surface states appears to be inhibited. This notion is supported by the fact that the surface imaging resolution, at normal bias voltages ($< \pm 2$ V) in the STM experiments at 77 K, was found to be considerably inferior to that at 300 K.

To further investigate the temperature dependence of the composite 2DEG-2DHG system, IV curves were recorded at various temperatures in the range from 80 to 180 K. For every temperature, 900 IV scans were recorded on a 10×10 grid (30×30 nm) and subsequently averaged. The result is shown in Fig. 5(a). Each IV scan was obtained from an initial set point voltage of -1 V, and took approximately 0.2 s. The most remarkable observation is the offset of the current at zero bias for temperatures below 180 K. This offset increases with decreasing temperature; see Fig. 5(b). This current offset is interpreted as resulting from a negative charging of the sample during the hold time at -1 V, before the scan is carried out.

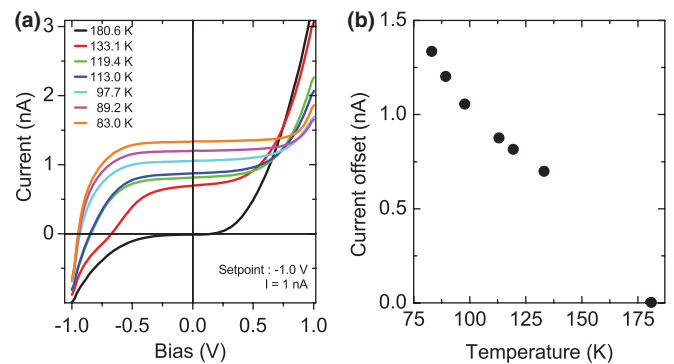


FIG. 5. (Color online) (a) Temperature dependent IV curves of the STO(001)/2LAO/1STO heterostructure recorded from 83 to 180 K. (Set point voltage $V = -1.0$ V and tunnel current $I = 1$ nA). (b) Current offset at zero bias for various temperatures.

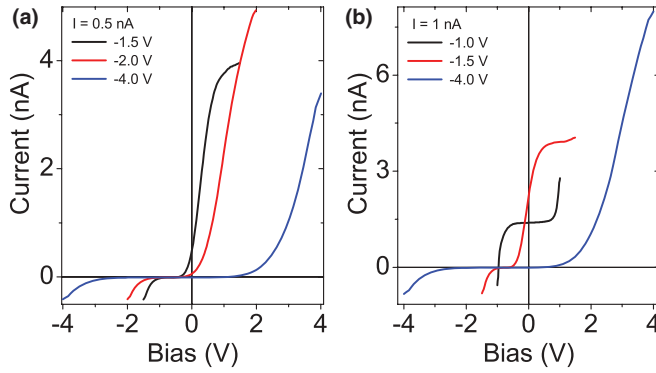


FIG. 6. (Color online) IV curves of the STO(001)/2LAO/1STO heterostructure recorded at 77 K with tunnel current set points of (a) 0.5 and (b) 1.0 nA.

During the IV scan, this charging is countered by a positive current flow to the sample.

This suggests that for decreasing temperatures the depletion of electrons in the upward shifted O $2p$ band cannot be replenished from the underlying interface, and hence the STO capping layer is positively charged with respect to the tip. Since no evidence for a Coulomb gap and a Coulomb staircase is observed in IV curves, the charging energy ($e^2/2C$) must be substantially larger than the thermal energy kT .^{26,27} The latter implies that the capacitance C must be significantly larger than 10^{-17} F. Decreasing the sample bias set point and scanning voltage to a value below -2 V does not result in charging of the top layer [see Figs. 6(a) and 6(b)]. Thus electrons that tunnel from filled states which are located more than 2 eV below the Fermi level of the STO capping layer can be replenished by the underlying interface at the substrate. Prolonged scanning at a voltage in the band gap region leads to a gradual increase of the decharging current (see Fig. 7). Moreover, increasing the set-point current shifts the charging current to higher values, but the decharging current at zero bias remains unaltered as shown in Fig. 7.

IV. DISCUSSION

The structural phase transition in STO from a cubic to a tetragonal phase may play a role in the fact that the phonon-assisted tunneling to the surface states is hampered by stiffening of the phonons. This phase transition is driven by the condensation of a zone corner phonon which involves the rotation of the oxygen octahedra.²⁸ Moreover, it is known that this phase transition must be treated very differently in

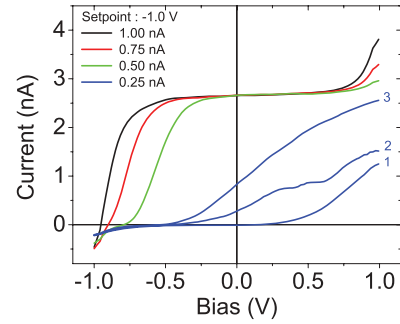


FIG. 7. (Color online) IV curves of the STO(001)/2LAO/1STO heterostructure recorded subsequently at 77 K with variable tunnel current set points of 0.25 (1,2,3: first curve 1 was recorded, followed by curves 2 and 3, respectively), 0.50, 0.75, and 1.0 nA and sample bias -1.0 V.

the near-surface region than in the bulk of the crystal. For instance the order parameter increases when the surface is approached from the interior of the crystal.²⁹ Salman *et al.*³⁰ found that the structural phase transition of STO occurs at a much higher temperature near the surface (150 K) as compared to the bulk (105 K), which would be in line with the observation of a reduced accessibility of the surface states below this temperature.

We have studied the electronic structure of the surface of the perovskite STO(001)/2LAO/1STO system with variable temperature scanning tunneling spectroscopy. At 300 K a band gap of ~ 1.0 eV is measured, whereas at 77 K the band gap widened to ~ 2.3 eV. The significant decrease in the band gap with increasing temperature is ascribed to an increased replenishment of charge from the underlying 2DEG to the surface 2DHG. At low temperatures the 2DHG can be positively charged by applying a negative sample bias voltage within the band gap region. At low temperatures the 2DHG can now be probed separately with the proposed experimental geometry, although the 2DEG is located less than 1 nm below. These local observations demonstrate the presence of two spatially separated 2D conducting sheets, one electronlike (2DEG) and the other holelike (2DHG), in epitaxial oxide heterostructures.

ACKNOWLEDGMENTS

This work is supported by the Netherlands Organization for Scientific Research (NWO) through VENI (M.H.), VIDI (A.B., G.R.), and VICI (H.H.) grants and by the Dutch Foundation for Fundamental Research on Matter (FOM) through the InterPhase program.

*m.huijben@utwente.nl

¹A. Ohtomo and H. Y. Hwang, *Nature (London)* **427**, 423 (2004).

²A. Brinkman, M. Huijben, M. Van Zalk, J. Huijben, U. Zeitler, J. C. Maan, W. G. Van der Wiel, G. Rijnders, D. H. A. Blank, and H. Hilgenkamp, *Nat. Mater.* **6**, 493 (2007).

³N. Reyren, S. Thiel, A. D. Caviglia, L. Kourkoutis, G. Hammerl, C. Richter, C. W. Schneider, T. Kopp, A.-S. Rüetschi, D. Jaccard,

M. Gabay, D. A. Muller, J.-M. Triscone, and J. Mannhart, *Science* **317**, 1196 (2007).

⁴M. Huijben, A. Brinkman, G. Koster, G. Rijnders, H. Hilgenkamp, and D. H. A. Blank, *Adv. Mater.* **21**, 1665 (2009).

⁵C. Cen, S. Thiel, J. Mannhart, and J. Levy, *Science* **323**, 1026 (2009).

- ⁶G. L. Cheng, P. F. Siles, F. Bi, C. Cen, D. F. Bogorin, C. W. Bark, C. M. Folkman, J. W. Park, C. B. Eom, G. Medeiros-Ribeiro, and J. Levy, *Nat. Nanotech.* **6**, 343 (2011).
- ⁷G. Herranz, M. Basletić, M. Bibes, C. Carrétéro, E. Tafra, E. Jacquet, K. Bouzehouane, C. Deranlot, A. Hamzić, J. M. Broto, A. Barthelemy, and A. Fert, *Phys. Rev. Lett.* **98**, 216803 (2007).
- ⁸A. Kalabukhov, R. Gunnarsson, J. Borjesson, E. Olsson, T. Claeson, and D. Winkler, *Phys. Rev. B* **75**, 121404 (2007).
- ⁹W. Siemons, G. Koster, H. Yamamoto, W. A. Harrison, G. Lucovsky, T. H. Geballe, D. H. A. Blank, and M. R. Beasley, *Phys. Rev. Lett.* **98**, 196802 (2007).
- ¹⁰A. S. Kalabukhov, Y. A. Boikov, I. T. Serenkov, V. I. Sakharov, V. N. Popok, R. Gunnarsson, J. Borjesson, N. Ljustina, E. Olsson, D. Winkler, and T. Claeson, *Phys. Rev. Lett.* **103**, 146101 (2009).
- ¹¹S. A. Chambers, M. H. Engelhard, V. Shutthanandan, Z. Zhu, T. C. Droubay, L. Qiao, P. V. Sushko, T. Feng, H. D. Lee, T. Gustafsson, E. Garfunkel, A. B. Shah, J.-M. Zuo, and Q. M. Ramasse, *Surf. Sci. Rep.* **65**, 317 (2010).
- ¹²P.R. Willmott, S.A. Pauli, R. Herger, C.M. Schlepütz, D. Martoccia, B.D. Patterson, B. Delley, R. Clarke, D. Kumah, C. Cionca, and Y. Yacoby, *Phys. Rev. Lett.* **99**, 155502 (2007).
- ¹³S. Thiel, G. Hammerl, A. Schmehl, C. W. Schneider, and J. Mannhart, *Science* **313**, 1942 (2006).
- ¹⁴M. Huijben, G. Rijnders, D. H. A. Blank, S. Bals, S. Van Aert, J. Verbeeck, G. Van Tendeloo, A. Brinkman, and H. Hilgenkamp, *Nat. Mater.* **5**, 556 (2006).
- ¹⁵J. Padilla and D. Vanderbilt, *Surf. Sci.* **418**, 64 (1998).
- ¹⁶R. Pentcheva, M. Huijben, K. Otte, W. E. Pickett, J. E. Kleibeuker, J. Huijben, H. Boschker, D. Kockmann, W. Siemons, G. Koster, H. J. W. Zandvliet, G. Rijnders, D. H. A. Blank, H. Hilgenkamp, and A. Brinkman, *Phys. Rev. Lett.* **104**, 166804 (2010).
- ¹⁷J. P. Eisenstein and A. H. MacDonald, *Nature (London)* **432**, 691 (2004).
- ¹⁸Y. Yoon, L. Tiemann, S. Schmult, W. Dietsche, K. von Klitzing, and W. Wegscheider, *Phys. Rev. Lett.* **104**, 116802 (2010).
- ¹⁹G. Koster, B. L. Kropman, A. J. H. M. Rijnders, D. H. A. Blank, and H. Rogalla, *Appl. Phys. Lett.* **73**, 2920 (1998).
- ²⁰See Supplemental Material at <http://link.aps.org/supplemental/10.1103/PhysRevB.86.035140> for detailed information on the controlled growth of heterostructures.
- ²¹V. Vonk, S. Konings, G. J. van Hummelen, S. Harkema, and H. Graafsma, *Surf. Sci.* **595**, 183 (2005).
- ²²R. M. Feenstra, J. A. Stroscio, and A. P. Fein, *Surf. Sci.* **181**, 295 (1987).
- ²³H. J. W. Zandvliet and A. van Houselt, *Ann. Rev. Anal. Chem.* **2**, 37 (2009).
- ²⁴M. Breitschaft, V. Tinkl, N. Pavlenko, S. Paetel, C. Richter, J. R. Kirtley, Y. C. Liao, G. Hammerl, V. Eyert, T. Kopp, and J. Mannhart, *Phys. Rev. B* **81**, 153414 (2010).
- ²⁵Z. Ristic, R. Di Capua, G. M. De Luca, F. Chiarella, G. Ghiringhelli, J. C. Cezar, N. B. Brookes, C. Richter, J. Mannhart, and M. Salluzzo, *Europhys. Lett.* **93**, 17004 (2011).
- ²⁶D. V. Averin and K. K. Likharev, *Mesoscopic Phenomena in Solids*, edited by B. L. Altshuler, P. A. Lee, and R. A. Webb (Elsevier, Amsterdam, 1991).
- ²⁷G. Schonberger, H. van Houten, and H. C. Donkersloot, *Europhys. Lett.* **20**, 249 (1992).
- ²⁸G. Shirane and Y. Yamada, *Phys. Rev.* **177**, 858 (1969).
- ²⁹D. P. Osterman, K. Mohanty, and J. D. Axe, *J. Phys. C* **21**, 2635 (1998).
- ³⁰Z. Salman, R. F. Kiefl, K. H. Chow, M. D. Hossain, T. A. Keeler, S. R. Kreitzman, C. D. P. Levy, R. I. Miller, T. J. Parolin, M. R. Pearson, H. Saadaoui, J. D. Schultz, M. Smadella, D. Wang, and W. A. MacFarlane, *Phys. Rev. Lett.* **96**, 147601 (2006).